Journal of Power Sources 195 (2010) 1071–1075

Contents lists available at ScienceDirect

Journal of Power Sources

journal homepage: www.elsevier.com/locate/jpowsour

Short communication

Synthesis of well-dispersed Pt/carbon nanotubes catalyst using dimethylformamide as a cross-link

J.B. Xu, T.S. Zhao*

Department of Mechanical Engineering, The Hong Kong University of Science and Technology, Clear Water Bay, Kowloon, Hong Kong SAR, China

ARTICLE INFO

Article history:
Received 12 June 2009
Received in revised form 5 August 2009
Accepted 19 August 2009
Available online 2 September 2009

Keywords:
Fuel cell
Catalyst
Platinum
Dimethylformamide
Carbon nanotube

ABSTRACT

In synthesizing carbon nanotubes supported catalysts, a significant challenge is how to deposit metal nanoparticles uniformly on the surface of carbon nanotubes due to the inherent inertness of carbon nanotube walls. This study reports a facile procedure using *N*,*N*-dimethylformamide as a dispersant, ligand and reductant, with which Pt nanoparticles can be deposited uniformly on pristine carbon nanotubes. X-ray photoelectron spectroscopy measurements reveal that metallic Pt nanoparticles are successfully prepared with this method. Transmission electron microscopy and X-ray diffraction analyses confirm the formation of face-centered cubic crystal Pt particles with a size that ranges from 2.0 to 4.0 nm. The support-dependent catalytic properties of the prepared Pt catalyst are characterized by cyclic voltammetric studies of the formic acid electro-oxidation reaction. The results show that a pristine carbon nanotubes supported Pt catalyst has a higher catalytic activity than both carbon powder and modified carbon nanotubes supported catalysts.

1. Introduction

To increase their electrochemically active area, catalysts supported on high surface area materials, commonly carbons, are widely used in low-temperature fuel cells. Recent studies have indicated that the physical properties of carbon materials can greatly affect the electrochemical properties of a supported catalyst. It has been reported that a carbon support with a high surface area and good crystallinity can not only provide a high dispersion of catalyst nanoparticles, but also facilitate electron transfer, and thereby result in better cell performance [1,2]. As carbon nanotubes (CNTs) have high surface areas, unique physical properties and morphology, high electrical conductivity and appropriate size and hollow geometry, their use as an electrocatalyst support material has received attention [3–5].

In synthesizing CNTs-supported catalysts, one of the most challenging tasks is how to deposit metal nanoparticles uniformly on the outer surface of CNTs due to the inertness of CNT walls [6]. To date, the most established protocol for the immobilization of catalyst particles on CNTs has been the so-called two-step method. This involves generating functional groups on the sidewalls first, mostly by harsh oxidative treatments, and then depositing metal nanoparticles on the activated surfaces [7]. Such surface functionalization provides an avenue for metal precursors to correlate with CNTs and prompts the deposition of metal on the outer walls. This functionalization can, however, cause defects on the surface of CNTs and lower their conductivity. Therefore, there exists a need to develop a simple and effective synthetic route that not only provides well-dispersed metal nanoparticles but also maintains a certain degree of control of particle size and size distribution on pristine CNTs.

A critical step in the synthesis of CNTs-supported composites is the preparation of a suspension of homogeneously isolated CNTs that can be accessed by different ions to make nanocomposites. Ultrasonication in solvents is usually a primary step for producing homogeneous and relatively aggregate-free dispersions. The dispersant used needs to overcome the strong van der Waals force between CNTs to resist their reagglomeration. Ham et al. [6] illustrated that solvents with high values of the dispersion component of the Hildebrand solubility parameter are the best for making homogeneous and agglomerate-free dispersions of CNTs. In this regard, *N*,*N*-dimethylformamide (DMF) proves to be better than ethanol, water, acetone and methanol for making CNTs dispersions. In this study, DMF is used as the bifunctional solvent, which acts as both a dispertant for CNTs and a ligand for Pt ions for the preparation of CNTs-supported Pt nanoparticles. In this route, DMF serves as a cross-link between the CNTs and the Pt ions that are expected to result in well-dispersed Pt nanoparticles on the outer surface of pristine CNTs.

Our previous work [8,9] has shown that Pt–Au and Pt–Ag nanoparticles with a narrow size distribution could be prepared using DMF as the reductant. Since, however, DMF is not an effective reductant for the metallic state Pt preparation at room temperature,

* Corresponding author. Tel.: +852 2358 8647.
E-mail address: metzhao@ust.hk (T.S. Zhao).

0378-7753/$ – see front matter © 2009 Elsevier B.V. All rights reserved.
doi:10.1016/j.jpowsour.2009.08.078

microwave (MW) heating is adopted in this work for the synthesis of the metallic Pt nanoparticles in DMF solution [10,11]. The catalytic properties of the prepared catalysts are characterized by cyclic voltammetry (CV) of the formic acid electro-oxidation reaction.

2. Experimental

2.1. Materials

All of the chemicals used were of analytical grade. Hexachloroplatinic acid was purchased from Aldrich. DMF, ethanol, formic acid, perchloric acid and potassium chloride (all from Merck KGaA) were used as-received. Vulcan XC-72 carbon powder (20–40 nm in size) was procured from E-TEK Company. Multi-walled carbon nanotubes with diameters 10–20 nm were obtained from Shenzhen Nanotech Co. Ltd., China. 5 wt.% Nafion solution was received from Dupont and used as-received.

2.2. MWNTs pretreatment

Well-established pretreatment processes were utilized to functionalize the CNTs [7]. Briefly, the CNTs were dispersed in 70% HNO_3 and subjected to ultrasonication for 10 min and refluxed at 120 °C for 4 h in order to reduce impurities such as the metal catalyst and amorphous products during the synthetic process. Surface functionalization of the CNTs was accomplished with a 4.0 M H_2SO_4–HNO_3 (1:1 v/v) mixture for 4 h under refluxing conditions.

2.3. Sample preparation

The carbon powder supported platinum nanoparticles were prepared as follows: 20 mL of 10 mM DMF coordinated Pt^{4+} complex precursor was mixed with 91 mg of carbon powder and ultrasonicated for 40 min to obtain a homogeneous solution. The mixture was introduced into a microwave oven (800 W, 2.45 GHz) and heated for 2 min at a specified fraction of the maximum microwave power, during which 20 mL DI water was added. After precipitation naturally, the supernatant solution was decanted and precipitated nanocomposites were washed several times with ethanol and water and dried at 70 °C in oven (Pt loading: 30 wt.%). The Pt black and the pristine carbon nanotubes (p-CNTs) and modified carbon nanotubes (m-CNTs) supported Pt nanoparticles were prepared via the same method (for Pt black, the precursor was 3 mM).

2.4. Preparation of working electrode

A glassy carbon electrode (GCE) (Taizhou Electroanalytical Instrument Factory, China, 4 mm in diameter) was polished to a mirror finish with 0.05 μm alumina suspension before each experiment and served as an underlying substrate of the working electrode. The catalyst ink was prepared by ultrasonically dispersing 10 mg of 30 wt.% of Pt/C, Pt/p-CNTs and Pt/m-CNTs in 1.9 mL of ethanol, to which 0.1 mL of 5 wt.% Nafion solution was added, and the dispersion was ultrasonicated for 30 min to obtain a homogeneous solution. A quantity of 9 μL of the dispersion was pipetted on the top of the GCE and dried in air to yield a metal loading of 108 $\mu g\,cm^{-2}$.

2.5. Characterization methods

Transmission electron microscopy (TEM) images were obtained by using a high-resolution JEOL 2010F TEM system operating with a LaB6 filament at 200 kV. The samples were dispersed in ethanol under sonication, dropped on the carbon-coated grid, and then imaged. The X-ray diffraction (XRD) patterns of the Pt/C, Pt/p-CNTs and Pt/m-CNTs catalysts were obtained with a Philips powder diffraction system (model PW 1830) using a Cu Kα source that operated at 40 keV at a scan rate of $0.025^\circ\,s^{-1}$. The surface characterization was carried out by the XPS technique, which was equipped with a Physical Electronics PHI 5600 multi-technique system using Al monochromatic X-ray at a power of 350 W. The survey and regional spectra were obtained by passing energy of 187.85 and 23.5 eV, respectively.

2.6. Electrochemical measurements

Electrochemical measurements were carried out by CV using a potentiostat (EG&G Princeton, model 273A). A conventional, three-electrode cell consisting of a GCE with an area of 0.125 cm^2 as the working electrode, Pt foil as the counter electrode, and a Ag/AgCl electrode as the reference electrode was used. The reference electrode was placed in a separate chamber, which is located close to the working electrode through a Luggin capillary tube. The CV experiments were performed in 0.5 M $HClO_4$ solution containing 0.25 M HCOOH at a scan rate of 50 $mV\,s^{-1}$. Solutions were prepared from analytical grade reagents and DI water. All experiments were performed at room temperature in nitrogen-saturated solutions. In all experiments, stable CV curves were recorded after scanning for 20 cycles in the potential region from −0.2 to 1.0 V in 0.5 M $HClO_4$ solution.

3. Results and discussion

3.1. Physicochemical characterization

Fig. 1 displays representative TEM images of Pt black and Pt/p-CNTs samples. Fig. 1a reveals that these Pt nanoparticles are spherical in shape and well-separated from each other, which is be further confirmed by the corresponding TEM image shown in Fig. 1b. Evaluation of the characteristic diameter of the Pt particles from an ensemble of 150 particles in an arbitrarily chosen area of the high-resolution TEM (HRTEM) images results in a narrow size distribution that ranges from 2.5 to 3.2 nm with an average value of 2.8 nm. Since, it has been demonstrated that the most favorable particle size for Pt-based electrocatalysts is in the range of 2.0–4.0 nm [12,13], this result indicates that DMF is an excellent reductant for the preparation of Pt-based electrocatalysts. In addition, DMF is an effective solvent for the dispersion of carbon nanotubes. Hence, DMF is used as the dispersant and reductant for the preparation of the pristine carbon nanotubes supported Pt catalyst. Typical TEM images of Pt/p-CNTs are presented in Fig. 1c and d. It is seen that the CNTs are covered with a continuous Pt nanoparticle, which extends the overall length of CNTs. This observation suggests that DMF can serve as a cross-link for Pt ions and pristine CNTs and there by induce well-dispersed Pt nanoparticles with a narrow particle size distribution (3.0–4.0 nm) on the outer surface of CNTs.

XPS was employed to analyze the valence state of the carbon-supported Pt nanoparticles. Regional Pt 4f spectra of Pt/C, Pt/p-CNTs and Pt/m-CNTs samples are given in Fig. 2. The Pt 4f spectra show a doublet containing a low-energy band (Pt $4f_{7/2}$) and a high-energy band (Pt $4f_{5/2}$) at 71.2 and 74.5 eV for Pt/p-CNTs and 71.3 and 74.6 eV for Pt/C and Pt/m-CNTs, respectively, indicating the existence of metallic state Pt [8]. Thus it is concluded that metallic Pt nanoparticles are successfully prepared in DMF though microwave radiation.

Fig. 3 shows the XRD scans of the Pt/C, Pt/p-CNTs and Pt/m-CNTs. The pattern of the supported Pt samples exhibits diffraction features that are consistent with face-centered cubic (fcc) cells having nearly identical lattice constants of 3.9384, 3.9194 and 3.9289 Å,

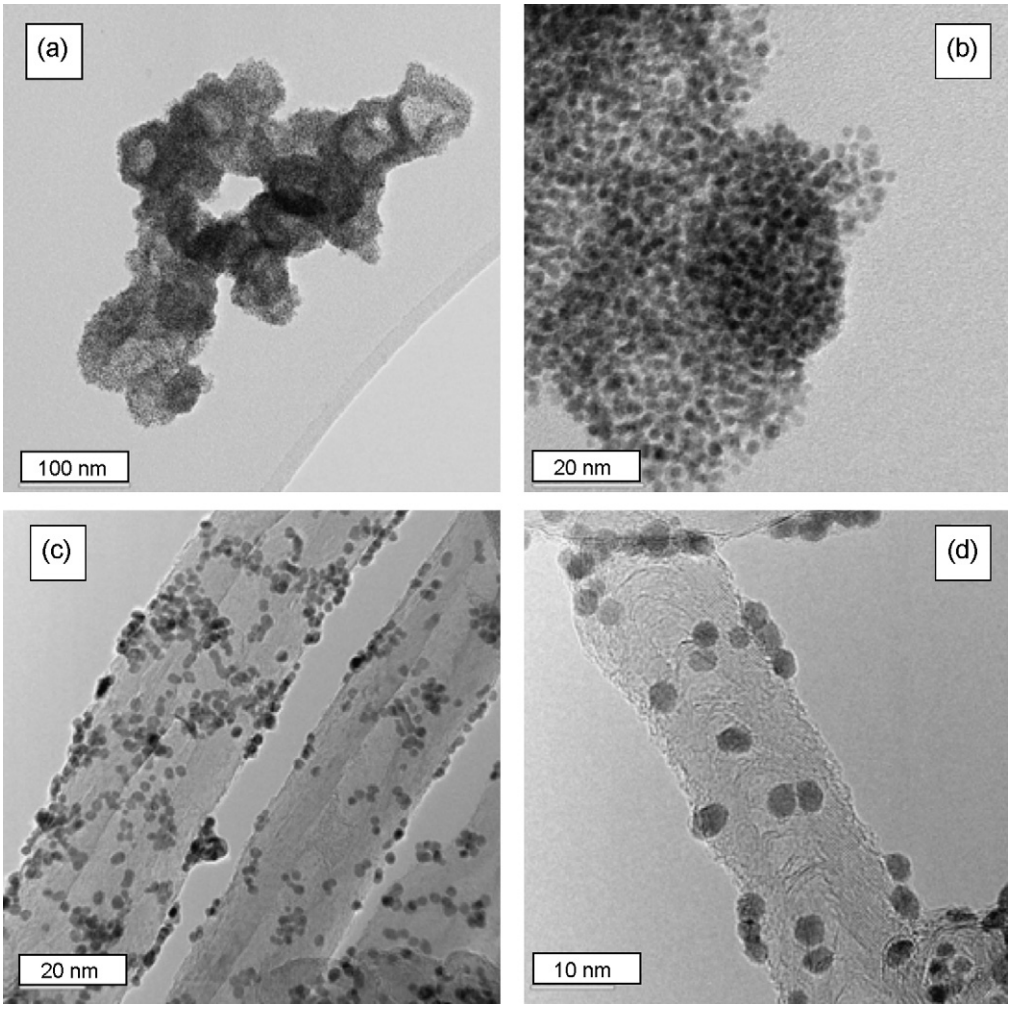

Fig. 1. TEM images of Pt black (a and b) and Pt/p-CNTs (c and d).

respectively. Furthermore, the existence of sharp diffraction peaks (0 0 2) around a 2θ value at 26° demonstrates the crystalline nature of CNTs. Hence, CNTs can act as a good conductive substrate and influence the crystalline nature of the Pt particles that are dispersed over them. In the case of carbon, at the same 2θ value very broad peaks appear and conform the amorphous nature of the Vulcan XC-72 carbon. In the preparative process of the supported Pt catalysts, all the parameters are maintained in an identical way to ensure that

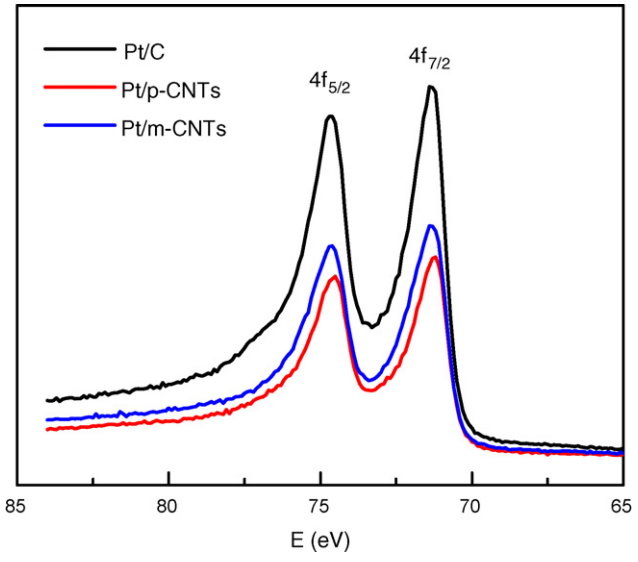

Fig. 2. Pt 4f XPS spectra of Pt/C, Pt/p-CNTs and Pt/m-CNTs.

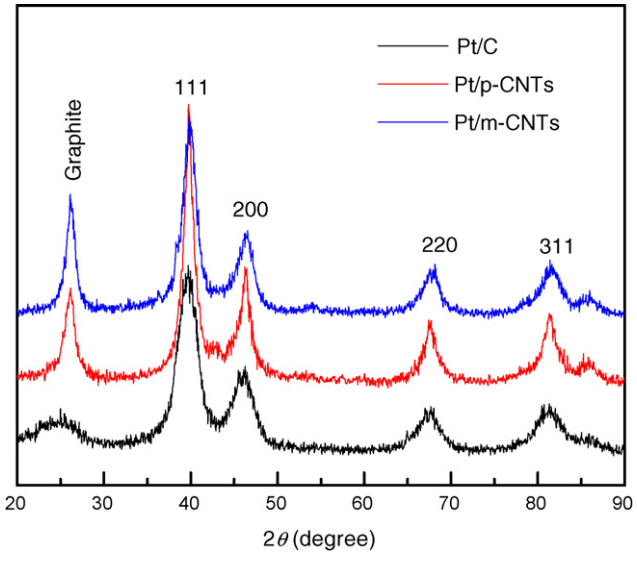

Fig. 3. XRD pattern of Pt/C, Pt/p-CNTs and Pt/m-CNTs samples.

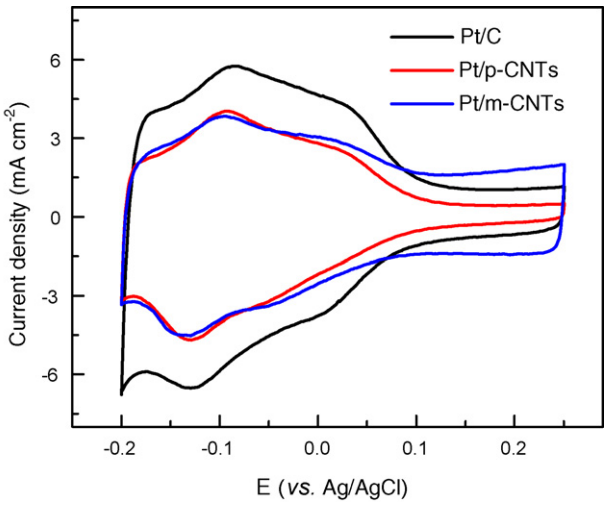

Fig. 4. CV curves of Pt/C, Pt/p-CNTs and Pt/m-CNTs catalysts in 0.5 M $HClO_4$ at sweep rate of 50 mV s^{-1}.

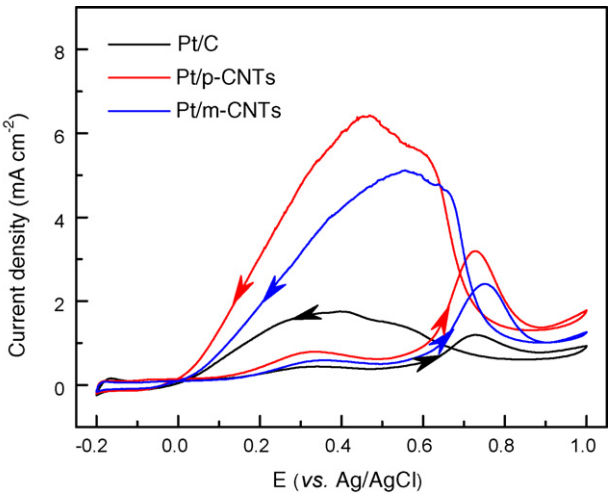

Fig. 5. CV curves of Pt/C, Pt/p-CNTs and Pt/m-CNTs catalysts in 0.5 M $HClO_4$ containing 0.25 M HCOOH at sweep rate of 50 mV s^{-1}. (For interpretation of the references to color in this figure legend, the reader is referred to the web version of the article.)

the loading, dispersion, and size of the Pt particles are essentially the same both on carbon and on CNTs. As compared with Pt/C and Pt/m-CNTs, the sharper diffraction peaks for Pt particles on p-CNTs reflect the larger average size due to the high crystalline grade of Pt. The average particle size of Pt/p-CNTs catalysts is 3.6 nm, as calculated from the broadening of the (2 2 0) diffraction peaks using Scherrer's equation [4]:

$$d = \frac{0.9\lambda}{B_{2\theta}\cos\theta_{\max}} \quad (1)$$

where λ is the wavelength of the X-ray (1.54056 Å), θ is the angle at the maximum of the peak, and $B_{2\theta}$ is the width of the peak at half-height. The mean particle size for Pt/C and Pt/m-CNTs is 3.2 and 3.5 nm, respectively.

3.2. Electrochemical characterization

The electrochemically active surface (EAS) areas of the as-synthesized catalysts were determined by means of CV over the potential range of −0.2 to 0.25 V in 0.5 M $HClO_4$ at a sweep rate of 50 mV s^{-1}. As can be seen in Fig. 4, the Pt/C, Pt/p-CNTs and Pt/m-CNTs have similar voltammetric features such as a polycrystalline Pt electrode with adsorption and desorption of hydrogen peaks in the voltammograms at potentials from −0.20 to 0.13 V [14]. Although the catalysts have the same elemental composition and metal loading, the Pt/C catalyst exhibits a higher hydrogen adsorption/desorption peak than the Pt/p-CNTs and Pt/m-CNTs catalysts. This demonstrates that the electrochemically active surface area of Pt/C is larger than that of Pt/p-CNTs and Pt/m-CNTs. This funding is consistent with XRD analysis that showed that Pt nanoparticles supported on carbon have a smaller size compared with Pt/p-CNTs and Pt/m-CNTs. The electrochemically active surface area of the three catalysts can be calculated from the CV curves by means of the following equation [15]:

$$\mathrm{EAS} = \frac{Q_H}{L_{Pt} q_H^0} \quad (2)$$

where Q_H is the integrated area of the hydrogen desorption (μC), L_{Pt} is the loading of Pt on the working electrode (mg), and q_H^0 is the charge for monolayer hydrogen adsorption on Pt 210 (μC cm^{-2}). The EAS areas of the Pt/C, Pt/p-CNTs and Pt/m-CNTs catalysts are 84.0, 58.5, 32.9 m^2 g^{-1}, respectively.

The support-related catalytic activities for formic acid oxidation on the Pt/C, Pt/p-CNTs and Pt/m-CNTs catalysts were characterized by CV performed in an electrolyte solution of 0.5 M $HClO_4$ and 0.25 M HCOOH. The results are shown in Fig. 5. To avoid the particle size effect, the reported current is normalized to the EAS. It can be seen that the formic acid electro-oxidation on the Pt/C electrode (the black line) Exhibits two anodic peaks in the forward scan. The first small anodic peak (~0.35 V) is attributed to the direct oxidation of formic acid to CO_2 on the remaining sites unblocked by intermediary species. The second peak and gradual increase of anodic current up to about 0.72 V are related to the oxidation of adsorbed intermediary species (CO), which releases the free surface sites for the subsequent direct oxidation of formic acid. In the backward scan, a bulk HCOOH oxidation peak, appears and occurs at approximately the same potential as the first anodic peak [16,17]. A similar situation is observed for the Pt/p-CNTs electrode. By comparison, the Pt/p-CNTs electrode (the red line) exhibits enhanced catalytic activity for formic acid oxidation relative to the Pt/C electrode. It can been seen in Fig. 5 that the first peak in the forward scan occurs at ~0.33 V, this negative shift of the peak potential indicates the higher catalytic activity of the Pt/p-CNTs towards formic acid electro-oxidation as compared with the Pt/C catalyst. This higher catalytic activity may be due to the high electronic conductivity of the CNTs that lowers the resistance to formic acid electro-oxidation. The same behaviour has been observed for the methanol electro-oxidation reaction on the CNTs-supported Pt-based catalysts [14,18]. As for the second peak, although no evident shift is observed, the peak current is higher than that for the Pt/C catalyst, and thereby demonstrates the higher catalytic activity. The CVs in Fig. 5 also reveal that the Pt/m-CNTs catalyst has a higher catalytic activity than Pt/C by yielding a higher peak current, but not as high as that for Pt/p-CNTs. In summary, these findings suggest that the CNTs show advantages over carbon power as a catalyst support for fuel cell applications. Moreover, pristine CNTs are better than modified types.

4. Conclusions

Uniform metallic Pt nanoparticles supported on pristine CNTs have been successfully prepared by using DMF as the dispersant, ligand and reductant. The support-dependent catalytic properties of Pt/p-CNTs have been analyzed by CV of the formic acid electro-oxidation reaction and are compared with that of the Pt/C. The results indicate that a Pt catalyst supported on pristine CNTs provides some advantages over carbon powder in terms of higher

catalytic activity for the formic acid oxidation reaction. The unique structure of CNTs makes them attractive as a catalyst support for fuel cells and the preparation method reported here offers a simple rout for the deposition of metal nanoparticles on the surface of pristine CNTs.

Acknowledgements

The work described was fully supported by a grant from the Research Grants Council of the Hong Kong Special Administrative Region, China (Project No. 623008).

References

[1] E. Antolini, Appl. Catal. B 88 (2009) 1.
[2] S.L. Knupp, W. Li, O. Paschos, T.M. Murray, J. Snyder, P. Haldar, Carbon 46 (2008) 1276.
[3] R.P. Raffaelle, B.J. Landi, J.D. Harris, S.G. Bailey, A.F. Hepp, Mater. Sci. Eng. B 116 (2005) 233.
[4] J.B. Xu, K.F. Hua, G.Z. Sun, C. Wang, X.Y. Lv, Y.J. Wang, Electrochem. Commun. 8 (2006) 982.
[5] M. Kaempgen, M. Lebert, N. Nicoloso, S. Roth, Appl. Phys. Lett. 92 (2008) 094103.
[6] H.T. Ham, Y.S. Choi, I.J. Chung, J. Colloid Interface Sci. 286 (2005) 216.
[7] R.Q. Yu, L.W. Chen, Q.P. Liu, J.Y. Lin, K.L. Tan, S.C. Ng, H. Chan, G.Q. Xu, T.S. Andyhor, Chem. Mater. 10 (1998) 718.
[8] J.B. Xu, T.S. Zhao, Z.X. Liang, L.D. Zhu, Chem. Mater. 20 (2008) 1688.
[9] J.B. Xu, T.S. Zhao, Z.X. Liang, J. Phys. Chem. C 112 (2008) 17362.
[10] W.C. Conner, G.A. Tompsett, J. Phys. Chem. B 112 (2008) 2110.
[11] P.S. Isabel, M.L.M. Luis, Adv. Funct. Mater. 19 (2009) 679.
[12] D. Zhao, B.Q. Xu, Angew. Chem. Int. Ed. 45 (2006) 4955.
[13] J.A.S. Bett, K. Kinoshita, P. Stonehart, J. Catal. 41 (1976) 124.
[14] J. Prabhuram, T.S. Zhao, Z.K. Tang, R. Chen, Z.X. Liang, J. Phys. Chem. B 110 (2006) 5245.
[15] J.W. Guo, T.S. Zhao, J. Prabhuram, R. Chen, C.W. Wong, Electrochim. Acta 51 (2005) 754.
[16] N. Kristian, Y.S. Yan, X. Wang, Chem. Commun. (2008) 353.
[17] S. Park, Y. Xie, M.J. Weaver, Langmuir 18 (2002) 5792.
[18] Y.Y. Mu, H.P. Liang, J.S. Hu, L. Jiang, L.J. Wan, J. Phys. Chem. B 109 (2005) 22212.